1   Title: SARS-CoV-2 infection severity is linked to superior humoral immunity against the spike

2

3   Jenna J. Guthmiller[1,12]*, Olivia Stovicek[1,12], Jiaolong Wang[1,12], Siriruk Changrob[1], Lei Li[1], Peter

4   Halfmann[2], Nai-Ying Zheng[1], Henry Utset[1], Christopher T. Stamper[3], Haley L. Dugan[3], William D.

5   Miller[4], Min Huang[1], Ya-Nan Dai[5], Christopher A. Nelson[5], Paige D. Hall[5], Maud Jansen[6], Kumaran

6   Shanmugarajah[7], Jessica S. Donington[7], Florian Krammer[8], Daved H. Fremont[5], Andrzej

7   Joachimiak[9,10], Yoshihiro Kawaoka[2], Vera Tesic[11], Maria Lucia Madariaga[7], Patrick C. Wilson[1,3]*

8

9   [1]Department of Medicine, Section of Rheumatology, University of Chicago, Chicago, IL 60637, USA

10   [2]Influenza Research Institute, Department of Pathobiological Sciences, School of Veterinary Medicine,

11   University of Wisconsin-Madison, Madison, WI, 53711

12   [3]Committee on Immunology, University of Chicago, Chicago, IL 60637, USA

13   [4]Department of Medicine, Section of Pulmonary and Critical Care Medicine, University of Chicago,

14   Chicago, IL 60637, USA

15   [5]Department of Pathology and Immunology and Center for Structural Genomics of Infectious

16   Diseases, Consortium for Advanced Science and Engineering, Washington University School of

17   Medicine, St. Louis, MO 63110, USA

18   [6]Department of Medicine, University of Chicago, Chicago, IL 60637, USA

19   [7]Department of Surgery, University of Chicago, Chicago, IL 60637, USA

20   [8]Department of Microbiology, Icahn School of Medicine at Mount Sinai, New York, NY 10029, USA

21   [9]Center for Structural Genomics of Infectious Diseases, Consortium for Advanced Science and

22   Engineering, University of Chicago, Chicago, IL 60667

23   [10]Structural Biology Center, X-ray Science Division, Argonne National Laboratory, Argonne, IL 60439,

24   USA

25   [11]Department of Pathology, University of Chicago, Chicago, IL 60637, USA

26   [12]These authors contributed equally

27   *Correspondence: jguthmiller@uchicago.edu; wilsonp@uchicago.edu

28   ABSTRACT: Severe acute respiratory syndrome coronavirus 2 (SARS-CoV-2) is currently causing a

29   global pandemic. The antigen specificity and kinetics of the antibody response mounted against this

30   novel virus are not understood in detail. Here, we report that subjects with a more severe SARS-CoV-

31   2 infection exhibit a larger antibody response against the spike and nucleocapsid protein and epitope

32   spreading to subdominant viral antigens, such as open reading frame 8 and non-structural proteins.

33   Subjects with a greater antibody response mounted a larger memory B cell response against the

34   spike, but not the nucleocapsid protein. Additionally, we revealed that antibodies against the spike are

35   still capable of binding the D614G spike mutant and cross-react with the SARS-CoV-1 receptor

36   binding domain. Together, this study reveals that subjects with a more severe SARS-CoV-2 infection

37   exhibit a greater overall antibody response to the spike and nucleocapsid protein and a larger memory

38   B cell response against the spike.

39

40

41   Entry of SARS-CoV-2 into host cells is mediated by surface trimeric spike protein via interaction

42   between the spike receptor-binding domain (RBD) and angiotensin-converting enzyme 2[1,2]. SARS-

43   CoV-2 expresses numerous potential antigens, including four structural proteins (spike, nucleocapsid

44   (N) protein, matrix and envelope protein), 16 nonstructural proteins/antigens (NSP1–NSP16), and

45   several accessory open reading frame (ORF) proteins, including ORF7 and ORF8[3,4]. To date, little is

46   known about the specificities and kinetics of antibodies elicited in response to this infection and how

47   coronavirus disease 2019 (COVID-19) severity relates to magnitude of the humoral immune

48   response.

49   To address this critically important knowledge gap, we collected plasma samples from 35

50   hospitalized acutely SARS-CoV-2 infected subjects and 105 convalescent subjects[5] (Supplemental

51   Tables 1 and 2). Plasma was tested against the spike, N protein, ORF7a, ORF8, and NSP3, NSP9,

52   NSP10, and NSP15 of SARS-CoV-2. Notably, all subjects within the acutely infected cohort were

53   hospitalized, whereas only 9% (8/105) of subjects in the convalescent cohort had been hospitalized

54   (Supplemental Tables 1 and 2). 89% of acutely infected subjects and 98% of convalescent subjects

55   had detectable antibodies against one or more SARS-CoV-2 antigens (Fig. 1a), with nearly all

56   subjects mounting a response against the spike and N protein (Fig. 1b). We further identified that

57   convalescent subjects mounted a predominant response against the RBD of the spike protein and the

58   RNA-binding domain of the N protein (Extended data Fig. 1a and b), suggesting these domains

59   contain the immunodominant epitopes of these antigens. A larger frequency of acutely infected

60   subjects mounted antibodies against ORF7a, ORF8, and NSP antigens (Fig. 1b, Extended data Fig.

61   1c) suggesting antibodies against these antigens are either short-lived or only induced by more

62   severe infection. Moreover, the anti-N protein antibody response preceded the antibody response

63   against the spike protein and was consistently higher across all time points, peaking between the 2nd

64   and 3rd week after the onset of symptoms and retracting between the 3rd and 4th weeks after symptom

65   onset (Fig. 1c and Extended data Fig. 1d). Furthermore, we found a strong positive correlation

66   between the anti-N protein and anti-spike IgG titers in both the acutely infected and convalescent

67   cohorts (Extended data 1e and f), indicating subjects who generally mounted a robust antibody

68   response upon SARS-CoV-2 infection tended to mount a robust response against both antigens.

69   Titers against both the spike and N protein persisted even 2+ months after symptom onset (Fig. 1c),

70   indicating the antibody response against these two antigens is stable amongst subjects with

71   symptomatic infection, a finding consistent with other reports[6,7]. We did not observe a statistical

72   difference in antibody titers against the spike and N protein by individual subjects in either the acute or

73   convalescent subject cohorts (Fig. 1d and e), likely due to dramatic subject-to-subject variation.

74   However, antibody titers against the spike and N protein were significantly higher than antibody titers

75   against ORF7a and ORF8 (Fig. 1d and e). Together, these data reveal the antibody response against

76   SARS-CoV-2 is largely driven against the spike and N protein and that the anti-N protein antibody

77   response precedes the response against the spike. The differences in the kinetics and magnitude of

78   the N protein response are potentially due to the differences in protein expression, as N protein

79   completely covers the entire viral genome, whereas a single virion only expresses ~26 trimers[8].

80   To understand the inter-subject variability within our cohorts, we performed hierarchical

81   clustering of subjects based on antibody titers against the spike, full length and RNA-binding domain

82   of N protein, ORF7a, and ORF8 antigens. From the acutely infected cohort, we identified three

83   clusters: high, mid, and low responders (Fig. 2a and Supplemental Table 3). Notably, the high

84   responder cluster subjects were further from the onset of symptoms at the time of sampling and

85   ultimately were hospitalized for a longer duration than those in the mid and low responder groups (Fig.

86   2b and c). We did not observe a statistical difference in age or sex between the three responder

87   groups (Extended data Fig. 2a and b). Over 25% of subjects in the high responder group had a

88   severe/highest CURB-65 score (Extended data Fig. 2c), a measure of pneumonia severity[9],

89   suggesting subjects in the high responder group had more severe infections. We further examined

90   which features of the humoral immune response were driving subjects to segregate into these three

91   clusters. Subjects within the high and mid responder groups robustly induced antibodies against the

92   spike protein, but the high responder subjects mounted a larger response to N protein relative to the

93   mid responder subjects (Fig. 2d-f). Additionally, subjects within the high and mid responder groups

94   were more likely to mount an antibody response against ORF8 and NSP antigens (Extended data Fig.

95 2d and e). The low responder group largely did not mount an antibody response against any of the

96 antigens tested (Fig. 2d-f and Extended Data Fig. 2d and e), although it is possible that plasma was

97 collected before the subjects mounted a significant antibody response. Our data reveal that acutely

98 infected subjects who were hospitalized for a longer duration mounted a larger antibody response

99 against N protein and were more likely to mount a response against other SARS-CoV-2 antigens.

100   The convalescent cohort also clustered into three distinct clusters based on the magnitude of

101 the antibody response against the spike and N protein (Fig. 3a and Supplemental Table 4), similar to

102 the acutely infected cohort (Fig. 2). To understand the relationship between infection severity and

103 antibody responses within the convalescent cohort, we scored subjects based on the severity and

104 duration of self-reported symptoms and whether subjects were hospitalized (Supplemental Table 5).

105 Notably, over 50% of subjects within the high responder group had a severe infection (Fig. 3b and

106 Extended data Fig. 3a), indicating infection severity is linked to increased antibody titers. Moreover,

107 subjects within the high responder group typically were older and male (Fig. 3c and d). Subjects within

108 each responder group had a similar duration of symptoms (Extended data Fig. 3b), and subjects

109 within all three groups had a similar amount of time to mount a response, as determined by the

110 number of days since symptoms onset at the time of donation (Extended data Fig. 3c). Unlike the

111 acutely infected cohort, subjects within the high responder group had higher titers against not only the

112 N protein, but also the spike and ORF8 antigens relative to subjects within the mid and low responder

113 groups (Fig. 3e and f, Extended data Fig. 3d and e), and were trending to be more likely to

114 seroconvert against at least one of the NSP antigens tested (Extended data Fig. 3f). Consistent with

115 these data, high and mid responder subjects had higher neutralizing titers than subjects in the low

116 responder cohorts (Fig. 3g). In combination with the acutely infected cohort, our data reveal subjects

117 with more severe infection are mounting a larger antibody response at both acute and convalescent

118 time points.

119   We next dissected the specificities of memory B cells (MBCs) induced by SARS-CoV-2

120 infection by performing B cell ELISpots on polyclonally stimulated peripheral blood mononuclear cells

121 (PBMCs) isolated from convalescent subjects. Notably, MBCs largely targeted the spike, whereas

5

122 very few MBCs targeted N protein or ORF8 (Fig. 4a). Additionally, subjects in the serum high

123 responder group mounted a larger MBC response against the spike than subjects in the mid and low

124 responder cohorts (Fig. 4b), with serum antibody titers against the spike positively correlating with the

125 magnitude of the anti-spike MBC response (Fig. 4c). Despite the observed differences in anti-spike

126 MBC responses between responder groups, we did not observe any differences in the anti-N protein

127 and anti-ORF8 MBC response in the three responder cohorts (Extended data Fig. 4a and b).

128 Together, these data indicate that the MBC response is largely directed against the spike protein, and

129 that the high serum responder group mounted both a larger secreted antibody and MBC response

130 upon SARS-CoV-2 infection.

131   SARS-CoV-2 has acquired a D614G mutation within the spike protein and viruses carrying this

132 mutation have since become the dominant circulating strain globally as of early April[10]. This mutation

133 is located on the interface between two subunits of the spike trimer and may impact stability of the

134 trimer[1]. As the subjects within our study were initially infected throughout March and into early April

135 (Supplemental Tables 1 and 2), they were likely infected with the D614 variant. We did not observe a

136 difference in antibody titers against the WT and D614G spike antigens within our acute cohort (Fig.

137 5a), suggesting the D614G epitope was not a major antigenic site. Strikingly, we identified that the

138 convalescent cohort mounted a larger response against the G614 variant than the WT D614 that they

139 were likely infected with (Fig. 5b), potentially due to the increased stability of the G614 variant[11].

140 Furthermore, we observed a strong positive correlation between D614 (WT) spike titers and G614

141 titers, indicating antibodies against the WT strain likely protect against the new G614 variant (Fig. 5c).

142 These data indicate that the region that encompasses the D614G mutation is not immunodominant or

143 does not affect the antigenicity of epitopes at or near this site. We also examined whether antibodies

144 targeting the RBD of the spike protein cross-reacted with the RBD proteins of other pandemic threat

145 coronaviruses, including SARS-CoV-1 and Middle East respiratory syndrome (MERS) CoV. We found

146 a positive correlation between antibody titers against the SARS-CoV-2 RBD and the SARS-CoV-1

147 RBD, but not the MERS-CoV RBD (Fig. 5d and e). When divided by responder groups (Fig. 2 and 3),

148 subjects in the high and mid responder groups had elevated titers against the SARS-CoV-1 RBD (Fig.

6

149 5f and g). These data show that subjects who mounted a larger response against the SARS-CoV-2

150 spike protein additionally mounted a larger antibody response against conserved epitopes that cross-

151 react with closely related coronaviruses.

152   Together, our study demonstrates that severity of SARS-CoV-2 infection is associated with an

153 increase in the magnitude and breadth of the ensuing humoral immune response. Notably, we

154 identified the antibody response is largely mounted against the spike and N proteins, with the

155 magnitude and kinetics of the anti-N protein antibody response outpacing the antibody response

156 against spike. Although both proteins are highly expressed by coronaviruses, there is much more N

157 protein as it encapsulates the whole viral genomic RNA, which is nearly 30 kb in size. As N protein

158 dimer is projected to bind about 30 bp[12], there are likely 1000+ N proteins per virion. In sharp contrast,

159 there are only ~26 spike trimers per virion[8], suggesting the immunodominance towards N protein may

160 be related to antigen burdens. Likewise, subjects with more severe disease likely have increased viral

161 titers and free antigen in the lung lumen and draining lymph nodes, which could lead to increased

162 antibody titers against nearly all antigens tested. Therefore, epitope spreading of the antibody

163 response may be a factor of the amount of SARS-CoV-2 antigen present.

164   Subjects also mounted an antibody response against the accessory protein ORF8. ORF8 has

165 immunoregulatory properties including the ability to limit type I interferon responses[13,14] and

166 downregulate MHC-I presentation to CD8 T cells[15]. Antibodies targeting ORF8 may limit these

167 immunoregulatory properties, which could improve the host immune response and achieve better

168 clinical disease outcomes. Additionally, we identified antibodies against non-structural proteins

169 involved in viral replication, although antibodies against these antigens are unlikely to provide

170 protection, as these antibodies targeting NSPs would need to be inside of a live cell while virus is

171 replicating. Whether antibodies targeting discrete viral antigens other than the spike are neutralizing,

172 have Fc-mediated effector functions, or are protective during infection remains to be determined.

173   Our study revealed acutely infected subjects who mounted higher antibody response relative

174 to mid and low responder clusters tended to have higher pneumonia severity scores. Consistent with

175 this notion, convalescent subjects who had higher antibody titers were those subjects who had a more

7

176   severe infection. A recent report identified that subjects who succumbed to COVID-19 tended to

177   mount a larger antibody response against N protein relative to the spike, whereas convalescent

178   subjects tended to focus their antibody response on the spike protein[16]. However, our study identified

179   that subjects generally had similar antibody responses against the N protein and spike, and infection

180   severity was linked to an increase in antibody responses against both the spike and N protein.

181   Ultimately, our findings on the relationship between infection severity and increased titers against the

182   spike is consistent with a recent surveillance study performed in Iceland[6].

183   The best clinical predictors of the magnitude of the antibody responses and epitope spreading

184   within our convalescent cohort were age, sex, and hospitalization. Strikingly, the median age of the

185   high responder cluster was 10+ years greater than the mid and low responder clusters (48 years vs.

186   36 and 38, respectively). Older adults are more likely to be symptomatic and hospitalized with SARS-

187   CoV-2 infection[17,18], suggesting increased disease severity and sustained viral titers over a longer

188   period of time could lead to greater antibody titers against multiple viral antigens. Similarly, males

189   were more likely to be segregated into the higher responder group despite the common finding that

190   females generally mount higher antibody responses upon other viral infections and upon

191   vaccination[19]. Although there is no difference in incidence of COVID-19 in men and women, men have

192   a higher morbidity and mortality rate than women[20,21] and likely experience increased viral titers and

193   antigen persistence. Altogether, disease severity is the main clinical predictor of the magnitude of the

194   antibody response mounted against SARS-CoV-2, as men and older adults are more likely to be

195   hospitalized with COVID-19. It remains to be determined whether subjects with more severe disease

196   are more likely to be protected from reinfection with SARS-CoV-2.

197   Together, our data indicate more severe infection is linked to a larger magnitude of circulating

198   antibody and MBC response and increased viral antigen binding breadth across different viral

199   antigens. CD4 T cells are critical for driving antibody responses by mediating germinal center

200   selection of antigen specific B cells. Notably, CD4 T cells targeting multiple SARS-CoV-2 antigens

201   and the magnitude of the CD4 T cell response positively correlate with SARS-CoV-2 specific antibody

202   responses[22,23]. Moreover, subjects with more severe disease demonstrate an increased breadth and

8

203   magnitude of the memory CD4 T cell response[23], which could lead to the larger and broader antibody

204   response of subjects with more severe infection, as observed in our study. The increase in the

205   magnitude of the antibody response and MBC response in subjects with more severe infection could

206   be due to increased CD4 T cell responses, although this was not directly tested in our study.

207   However, subjects who succumbed to SARS-CoV-2 infection demonstrated a loss of germinal centers

208   and CD4 T follicular helper cells[24]. These data in conjunction with our study suggest that an

209   immunological balance will be needed to drive a sufficient secreted antibody response, MBC

210   differentiation, and memory T cell responses that could provide robust protection from reinfection

211   while preventing significant morbidity and mortality associated with SARS-CoV-2 infection.

9

212   **Methods**

213   **Study cohorts**

214   All studies were performed with the approval of the University of Chicago institutional review board

215   and University of Chicago and University of Wisconsin-Madison institutional biosafety committees.

216   Plasma samples from the acutely infected cohort were collected as residual samples submitted to the

217   University of Chicago Medicine Clinical Laboratories. Convalescent subjects were recruited to donate

218   one unit of blood for a convalescent plasma transfusion study, identified as clinical trial

219   NCT04340050. 3 ml of blood and the leukoreduction filter were provided to the Wilson laboratory. All

220   subjects in the acute and convalescent cohorts had PCR-confirmed SARS-CoV-2 infections.

221   **Recombinant proteins**

222   Plasmids for the SARS-CoV-2 RBD and spike were provided by Dr. Florian Krammer at Icahn School

223   of Medicine at Mount Sinai, and recombinant proteins were expressed in-house in HEK293F cells.

224   D614G spike protein, SARS-CoV-1 RBD, and MERS-CoV RBD were generated in-house and

225   expressed in HEK293F cells. ORF7a, ORF8, and full-length N proteins were cloned from the 2019-

226   nCoV/USA-WA1/2020 SARS-CoV-2 strain at Washington University. Proteins were expressed in

227   *Escherichia coli*, with N protein purified as a soluble protein and ORF7a and ORF8 oxidatively

228   refolded from inclusion bodies. NSP antigens and the RNA-binding domain of N protein were provided

229   by Dr. Andrzej Joachimiak at the Center for Structural Genomics of Infectious Diseases at the

230   University of Chicago and Argonne National Laboratory and were expressed in *Escherichia coli*.

231   **Enzyme-linked immunosorbent assay (ELISA)**

232   ELISAs performed in this study were adapted from previously established protocols[25,26]. Plasma

233   samples were heat-inactivated for 1 hour at 56°C. High protein-binding microtiter plates (Costar) were

234   coated with recombinant antigens at 2 µg/ml in phosphate-buffered saline (PBS) overnight at 4°C.

235   Plates were washed with PBS 0.05% Tween and blocked with 200 µl PBS 0.1% Tween + 3% milk

236   powder for 1 hour at room temperature. Plasma samples were serially diluted in PBS 0.1% Tween +

237   1% milk powder. Plates were incubated with serum dilutions for 2 hours at room temperature.

238   Horseradish peroxidase (HRP)-conjugated goat anti-human Ig secondary antibody diluted in PBS

10

239 0.1% Tween + 1% milk powder was used to detect binding of antibodies, and after a 1-hour

240 incubation, plates were developed with 100 µl SigmaFast OPD solution (Sigma-Aldrich), with

241 development reaction stopped after 10 minutes using 50 µl 3M HCl. Absorbance was measured at

242 490 nm on a microplate spectrophotometer (BioRad). To detect binding of specific antibody isotypes

243 and subclasses, ELISAs were performed using alternate secondary antibodies (Sigma-Aldrich;

244 Jackson ImmunoResearch; Southern Biotech). End point titers were extrapolated from sigmoidal 4PL

245 (where X is log concentration) standard curve for each sample. Limit of detection (LOD) is defined as

246 the mean plus 2-8 S.D. (depending on antigen) of the O.D. signal recorded using plasma from SARS-

247 CoV-2 negative human subjects. All calculations were performed in Prism 8 (GraphPad).

248 **Neutralization assays**

249 Neutralization assays were performed by a viral cytopathic effect assay (CPE) using the SARS-CoV-

250 2/UW-001/Human/2020/Wisconsin (UW-001), which was isolated from a mild human case in

251 Wisconsin. Plasma was diluted 1:5 and serially diluted 2-fold and was mixed with an equal volume of

252 virus (100 plaque-forming units) for a starting dilution of 1:10. The plasma/virus mixture was incubated

253 for 30 minutes at 37°C and added to TMPRSS2-expressing Vero E6 cells grown in 1x minimum

254 essential medium (MEM) supplemented with 5% FCS. Cells were incubated with plasma/virus mixture

255 for 3 days, and then were fixed, stained, and analyzed. CPE was observed under an inverted

256 microscope, and neutralization titers were determined as the highest serum dilution that completely

257 prevented CPE.

258 **Memory B cell stimulations and enzyme-linked immunospot assays (ELISpot)**

259 MBC stimulations were performed on peripheral blood mononuclear cells (PBMCs) collected from

260 subjects in the convalescent cohort. To induce MBC differentiation into antibody secreting cells, 1×10^6

261 PBMCs were stimulated with 10 ng/ml Lectin Pokeweed Mitogen (Sigma-Aldrich), 1/100,000 Protein A

262 from *Staphylococcus aureus*, Cowan Strain (Sigma-Aldrich), and 6 µg/ml CpG (Invitrogen) in

263 complete RPMI in an incubator at 37°C/5% CO_2 for 5 days. After stimulation, cells were counted and

264 added to ELISpot white polysterene plates (Thermo Fisher) coated with 4 µg/ml of SARS-CoV-2 spike

265   that were blocked with 200 µl of complete RPMI. ELISpot plates were incubated with cells for 16

266   hours overnight in an incubator at 37°C/5% CO_2. After the overnight incubation, plates were washed

267   and incubated with anti-IgG-biotin and/or anti-IgA-biotin (Mabtech) for 2 hours at room temperature.

268   After secondary antibody incubation, plates were washed and incubated with streptavidin-alkaline

269   phosphatase (Southern Biotech) for 2 hours at room temperature. Plates were washed and developed

270   with NBT/BCIP (Thermo Fisher Scientific) for 2-10 minutes, and reactions were stopped by washing

271   plates with distilled water and allowed to dry overnight before counting. Images were captured with

272   Immunocapture 6.4 software (Cellular Technology Ltd.), and spots were manually counted.

273   **Infection Severity Scoring and CURB-65 scoring**

274   For the acutely infected cohort, CURB-65[9] scores were calculated based on confusion, blood urea

275   nitrate levels, respiratory rate, blood pressure, and age of subjects. For the convalescent cohort, we

276   designed a severity scoring system (Supplemental Table 5) based on presence of 12 symptoms,

277   duration of symptoms, and hospitalization, with a maximum of 35 points possible. Symptoms were

278   scored based on presence or absence of 12 symptoms, severity (mild or moderate) of symptoms, with

279   a possibility of 17 points. Duration of symptoms was broken down based on the number of weeks of

280   symptoms. Hospitalized subjects were broken down based on oxygen supplementation and intensive

281   care unit (ICU) admission. The criteria for scoring and the classification of certain scores (mild,

282   moderate, severe, and critical infection) were determined before analyzing the data.

283   **Heatmaps, hierarchical clustering, and statistical analysis**

284   Heatmaps were generated by 'pheatmap' *R* package (version 1.0.12). Features and subjects were

285   clustered by the hierarchical clustering method implemented in the 'pheatmap' *R* package. Principal

286   component analyses (PCA) were performed using 'factoextra' *R* package (version 1.0.7). Subjects

287   were then visualized by their first two principal components (PC1 and PC2) on a 2D map. All

288   statistical analysis was performed using Prism software (Graphpad Version 8), JMP (SAS Institute

289   Version 15), or *R* (version 3.6.3). Specific tests for statistical significance used are indicated in the

290   corresponding figure legends. *P* values less than or equal to 0.05 were considered statistically

291   significant.

Acknowledgements

Author Contributions

J.J.G. designed and performed experiments, analyzed the data, and wrote the manuscript. O.S. and J.W. performed experiments, analyzed the data, and wrote the manuscript. S.C., N.Y.Z., H.U., M.H., Y.N.D., C.A.N, and P.D.H. generated recombinant antigens. J.J.G., S.C., N.Y.Z., H.U., C.T.S., and H.L.D. processed convalescent blood samples. J.J.G., O.S., and C.T.S. processed samples from acutely infected subjects. J.J.G., J.W., S.C., C.T.S., and H.L.D. performed and analyzed ELISpot assays. L.L. performed hierarchical clustering and PCA analyses. P.H. and Y.K. performed neutralization assays. J.J.G., W.D.M., and M.L.M. designed the scoring system for convalescent subjects. M.J., K.S., J.S.D., and M.L.M. orchestrated convalescent plasma study. F.K., D.H.F., and A.J. provided recombinant antigens or plasmids to express recombinant antigens. V.T. provided samples from acutely infected subjects and helped analyze data. P.C.W. supervised the work. All authors edited the manuscript.

Declaration of Interests

The authors declare no competing interests.
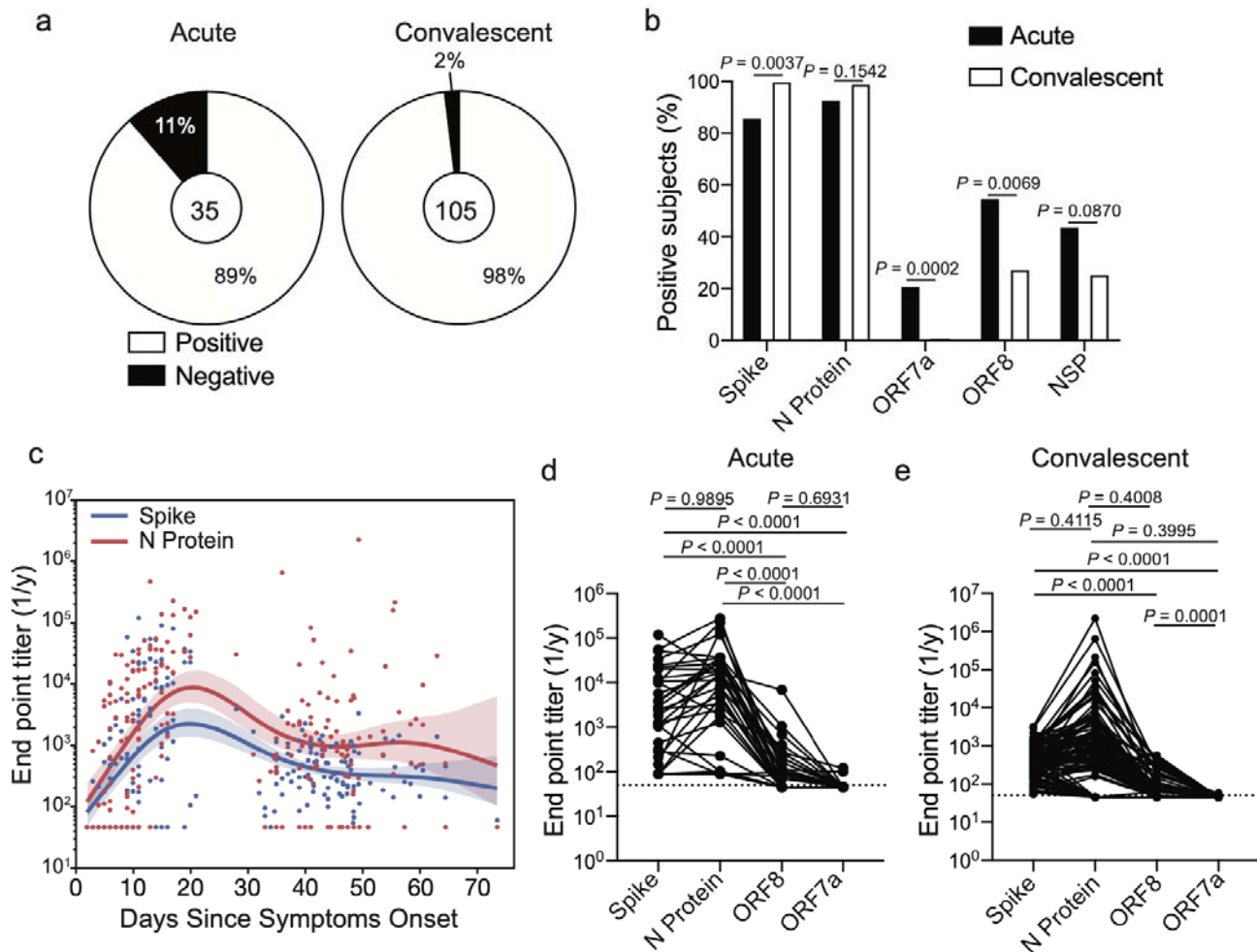
**Fig. 1: Antibody specificity and kinetics in SARS-CoV-2 infected subjects. a,** Proportion of subjects in the acutely infected and convalescent cohorts who have seroconverted to one or more SARS-CoV-2 antigens. Number in center represents the number of subjects tested in each cohort. **b,** Proportion of subjects in the acutely infected (n=35) and convalescent (n=105) cohorts binding spike, N protein, ORF7a, ORF8, or at least one NSP antigen. **c,** Kinetics of plasma antibodies against the spike and N protein based on the start of symptoms. Data are pooled from the acute (n=117) and convalescent cohorts (n=105). Lines represent the fitted lines for spike and N protein titers and the shaded region indicates confidence of fit of the fitted line. **d** and **e,** end point titers of antibodies targeting spike, N protein, ORF7a, and ORF8 in the acutely infected cohort (**d**; n=35) and convalescent cohort (**e**; n=105). Lines connect titers across one subject. Data in **b** were analyzed

14

330   using Fisher's exact tests for statistical analyses. Data in **d** and **e** were analyzed using paired non-

331   parametric Friedman tests. Dashed lines in **d** and **e** are the limit of detection.

332
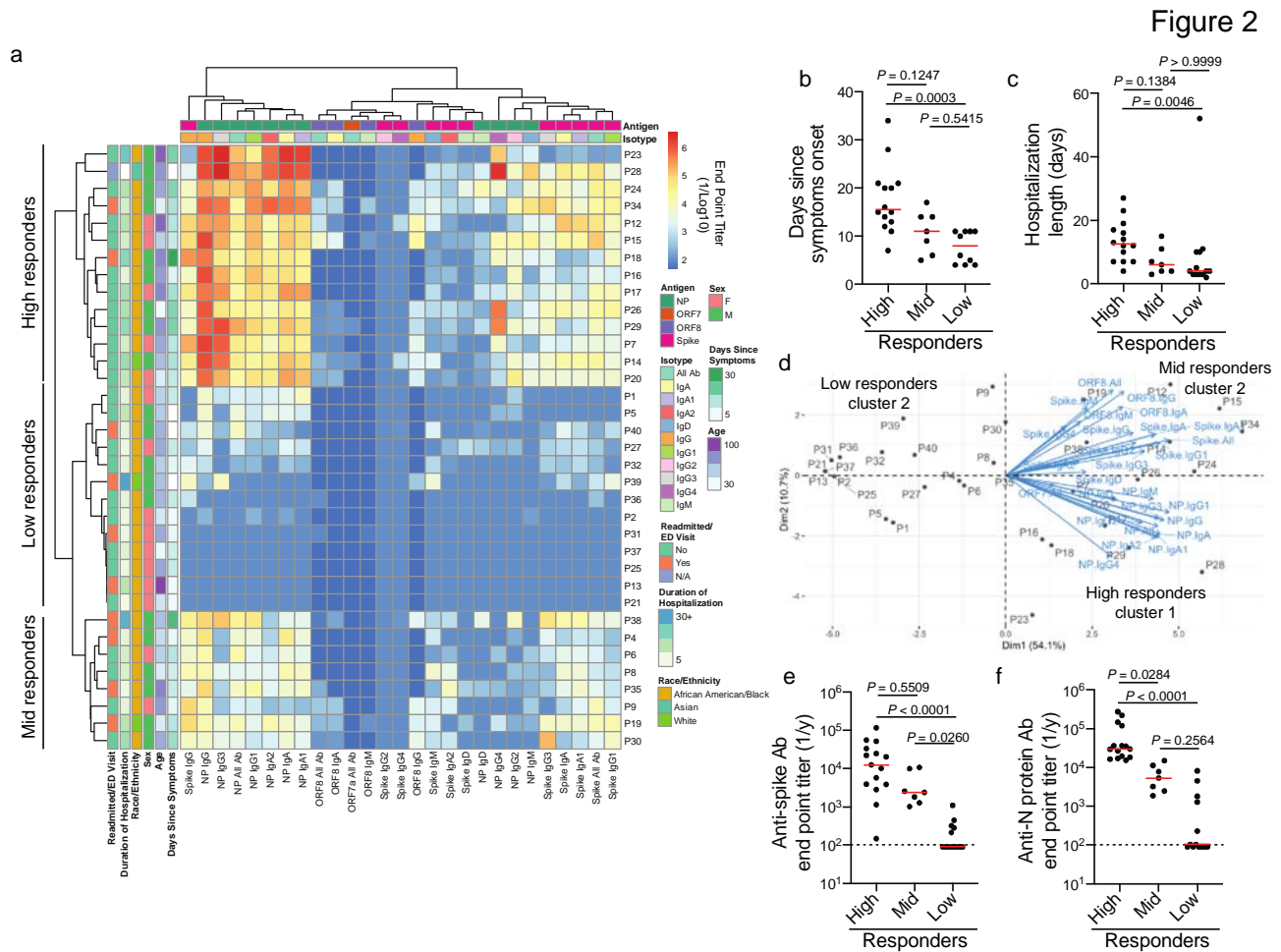
Fig. 2: **Acutely infected subjects with longer hospitalizations have a higher antibody response against N protein. a**, Heatmap of hierarchical clustering of acutely infected subjects (n=35) based on antibody binding specificity and antibody isotype/subclass. Subjects clustered into three distinct clusters: high (n=15), mid (n=7), and low (n=13) responders. **b** and **c**, days since symptom onset (**b**) and length of hospitalization (**c**) amongst subjects in the high, mid and low responder clusters. **d**, PCA biplot of subjects clustering based on distinct antibody binding features. **e** and **f**, total antibody titers against the spike (**e**) and N protein (**f**) amongst the high, mid, and low responder clusters. Data in **b**, **c**, **e**, and **f** were analyzed using unpaired non-parametric Kruskal-Wallis tests. Dashed lines in **e** and **f** are the limit of detection. Bars in **b**, **c**, **e**, and **f** represent the median.

Figure 3
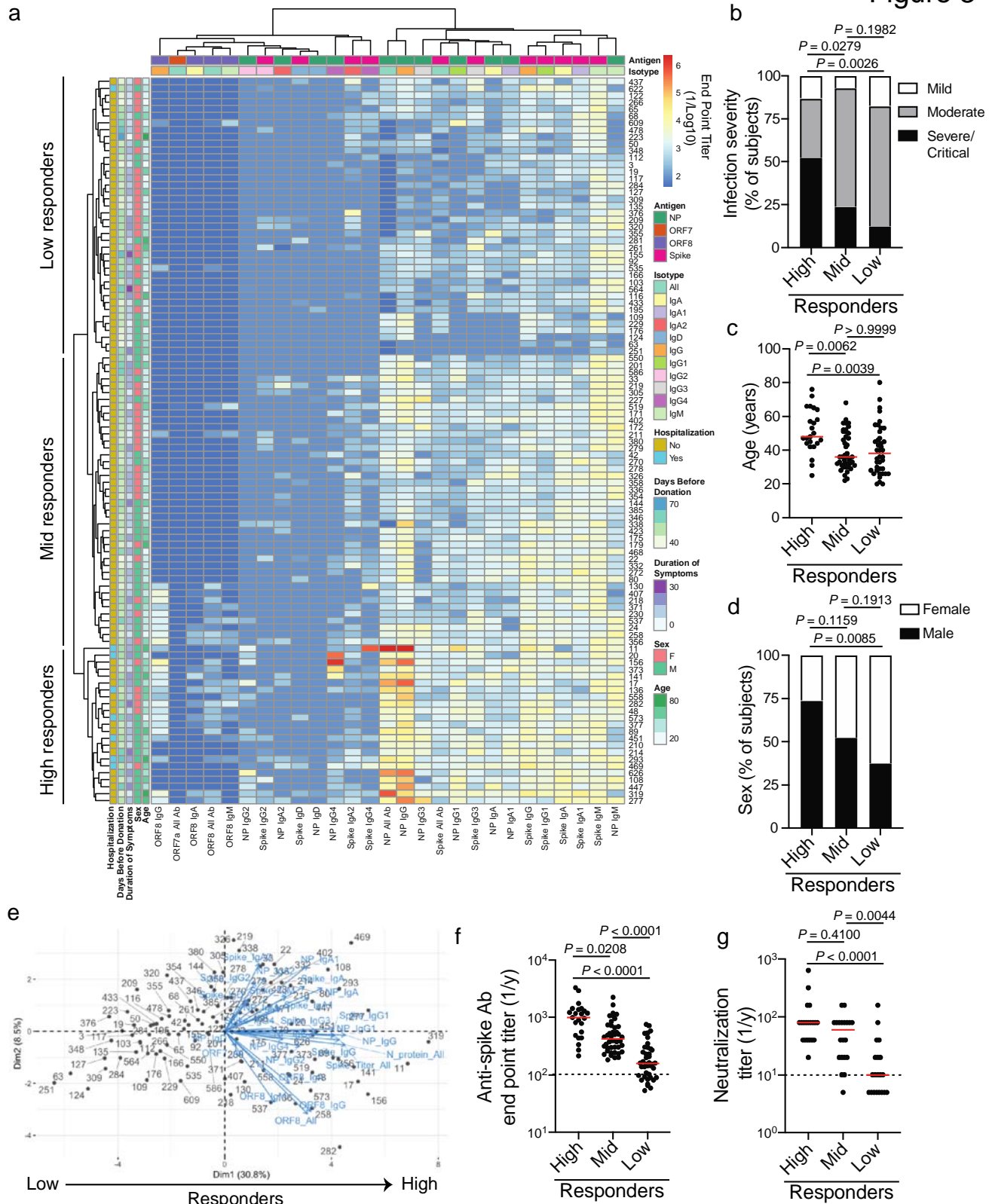
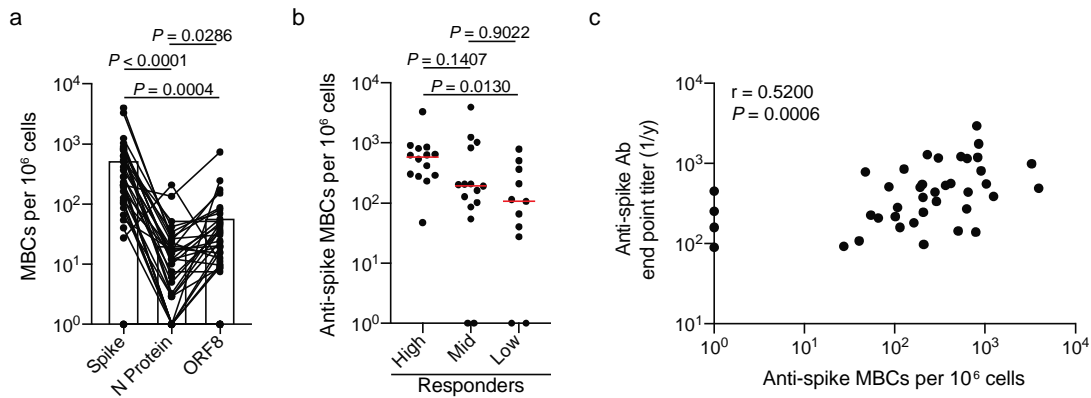**Fig. 3**: **Convalescent subjects with higher antibody responses against multiple SARS-CoV-2 antigens tended to have a more severe infection. a**, Heatmap of hierarchical clustering of

17

346   convalescent subjects (n=105) based on antibody binding specificity and antibody isotype/subclass.

347   Subjects clustered into three distinct clusters: high (n=23), mid (n=42), and low (n=40) responders. **b-**

348   **d**, infection severity (**b**), age (**c**) and sex (**d**) of subjects in the high, mid and low responder clusters. **e**,

349   PCA biplot of subjects clustering based on distinct antibody binding features. **f**, Total antibody titers

350   against the spike amongst the high, mid, and low responder clusters. **g**, Neutralization titer, as

351   determined by viral cytopathic effect, of 20 randomly selected samples from each of the high, mid,

352   and low responder clusters. Data in **f** and **g** were analyzed using unpaired non-parametric Kruskal-

353   Wallis tests. For **b-d**, data were analyzed using Fisher's exact tests. Dashed lines in **f** and **g** are the

354   limit of detection. Bars in **f** and **g** represent the median.

18

Figure 4

Fig. 4: MBC response is largely driven against the spike. a and **b**, PBMCs from convalescent donors were polyclonally stimulated and ELISpots were performed to assess the number of antigen-specific MBCs. **a**, Number of MBCs (antigen-specific MBCs per 10^6 cells) targeting the spike, N protein, or ORF8 (n=36). Lines connect antigen-specific MBCs across subjects. **b**, Number of spike targeting MBCs amongst the high (n=14), mid (n=15), and low responder (n=11) clusters. **c**, Spearman correlation of the number of anti-spike MBCs and anti-spike end point titers by individual (n=40). Data in **a** were analyzed using paired non-parametric Friedman tests. Data in **b** were analyzed using unpaired non-parametric Kruskal-Wallis tests. Data in **c** were analyzed by a non-parametric two-tailed Spearman correlation.

19
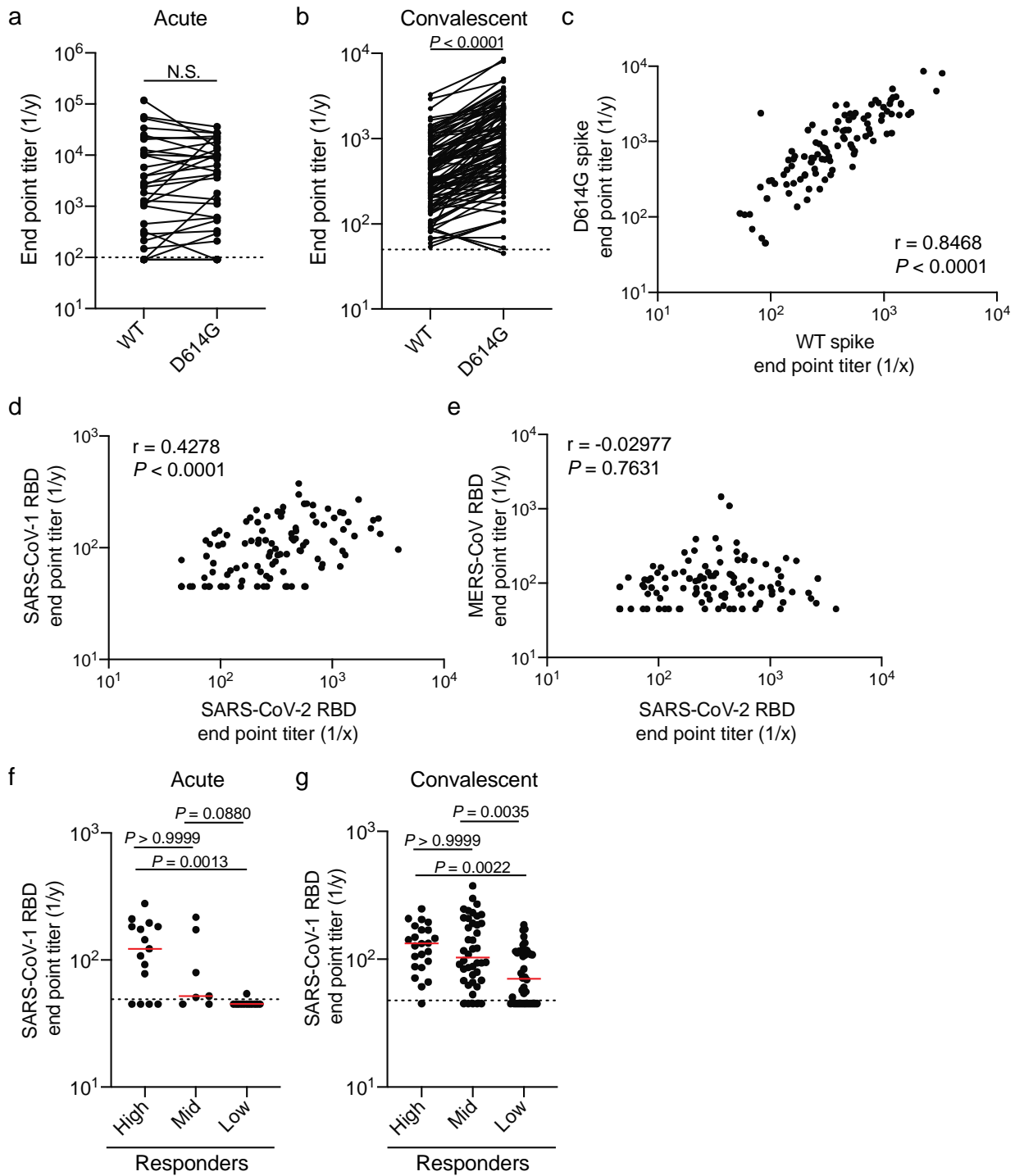
Fig. 5: **Antibody cross-reactivity to G614 spike mutant and SARS-CoV-1 and MERS-CoV RBD. a**

and **b**, End point titers of antibodies binding to the WT (D614) and mutant (D614G) SARS-CoV-2

spike protein from the acute (**a**; n=35) and convalescent (**b**; n=105) cohorts. **c**, Correlation of end

point titers against the WT (D614) and mutant (D614G) spike from the convalescent cohort (n=105). **d**

371   and **e**, correlation between SARS-CoV-2 RBD end point titers and SARS-CoV-1 RBD (**d**) or MERS-

372   CoV RBD (**e**) end point titers from convalescent subjects (n=105). **f** and **g**, SARS-CoV-1 RBD end

373   point titers amongst the high, mid, and low responder clusters from the acutely infected cohort (**f;** high

374   n=23, mid n=42, and low n=40) and the convalescent cohort (**g**; high n=23, mid n=42, and low n=40).

375   Data in **a** were analyzed using a two-tailed Wilcoxon matched-pairs signed rank test. Data in **b** were

376   analyzed using a two-tailed paired t-test. For **c-e**, data were analyzed using a two-tailed Pearson

377   correlation. Data in **f** and **g** were analyzed using unpaired non-parametric Kruskal-Wallis tests.

378   Dashed lines in **a**, **b**, **f** and **g** are the limit of detection. Bars in **f** and **g** represent the median.

379 References

380 1 Walls, A. C. *et al.* Structure, Function, and Antigenicity of the SARS-CoV-2 Spike
381 Glycoprotein. *Cell* **181**, 281-292 e286, doi:10.1016/j.cell.2020.02.058 (2020).
382 2 Letko, M., Marzi, A. & Munster, V. Functional assessment of cell entry and receptor usage for
383 SARS-CoV-2 and other lineage B betacoronaviruses. *Nat Microbiol* **5**, 562-569,
384 doi:10.1038/s41564-020-0688-y (2020).
385 3 Amanat, F. & Krammer, F. SARS-CoV-2 Vaccines: Status Report. *Immunity* **52**, 583-589,
386 doi:10.1016/j.immuni.2020.03.007 (2020).
387 4 Chan, J. F. *et al.* Genomic characterization of the 2019 novel human-pathogenic coronavirus
388 isolated from a patient with atypical pneumonia after visiting Wuhan. *Emerg Microbes Infect* **9**,
389 221-236, doi:10.1080/22221751.2020.1719902 (2020).
390 5 Madariaga, M. L. L. *et al.* Clinical predictors of donor antibody titer and correlation with
391 recipient antibody response in a COVID-19 convalescent plasma clinical trial. *medRxiv*,
392 2020.2006.2021.20132944, doi:10.1101/2020.06.21.20132944 (2020).
393 6 Gudbjartsson, D. F. *et al.* Humoral Immune Response to SARS-CoV-2 in Iceland. *N Engl J
394 Med*, doi:10.1056/NEJMoa2026116 (2020).
395 7 Rodda, L. B. *et al.* Functional SARS-CoV-2-specific immune memory persists after mild
396 COVID-19. *medRxiv*, doi:10.1101/2020.08.11.20171843 (2020).
397 8 Ke, Z. *et al.* Structures and distributions of SARS-CoV-2 spike proteins on intact virions.
398 *Nature*, doi:10.1038/s41586-020-2665-2 (2020).
399 9 Lim, W. S. *et al.* Defining community acquired pneumonia severity on presentation to hospital:
400 an international derivation and validation study. *Thorax* **58**, 377-382,
401 doi:10.1136/thorax.58.5.377 (2003).
402 10 Korber, B. *et al.* Tracking Changes in SARS-CoV-2 Spike: Evidence that D614G Increases
403 Infectivity of the COVID-19 Virus. *Cell*, doi:10.1016/j.cell.2020.06.043 (2020).
404 11 Zhang, L. *et al.* The D614G mutation in the SARS-CoV-2 spike protein reduces S1 shedding
405 and increases infectivity. *bioRxiv*, doi:10.1101/2020.06.12.148726 (2020).
406 12 Huang, Q. *et al.* Structure of the N-terminal RNA-binding domain of the SARS CoV
407 nucleocapsid protein. *Biochemistry* **43**, 6059-6063, doi:10.1021/bi036155b (2004).
408 13 Li, J. Y. *et al.* The ORF6, ORF8 and nucleocapsid proteins of SARS-CoV-2 inhibit type I
409 interferon signaling pathway. *Virus Res* **286**, 198074, doi:10.1016/j.virusres.2020.198074
410 (2020).
411 14 Lei, X. *et al.* Activation and evasion of type I interferon responses by SARS-CoV-2. *Nat
412 Commun* **11**, 3810, doi:10.1038/s41467-020-17665-9 (2020).
413 15 Zhang, Y. *et al.* The ORF8 Protein of SARS-CoV-2 Mediates Immune Evasion through
414 Potently Downregulating MHC-I. *bioRxiv*, 2020.2005.2024.111823,
415 doi:10.1101/2020.05.24.111823 (2020).
416 16 Atyeo, C. *et al.* Distinct Early Serological Signatures Track with SARS-CoV-2 Survival.
417 *Immunity*, doi:10.1016/j.immuni.2020.07.020 (2020).
418 17 Davies, N. G. *et al.* Age-dependent effects in the transmission and control of COVID-19
419 epidemics. *Nat Med*, doi:10.1038/s41591-020-0962-9 (2020).
420 18 Tenforde, M. W. *et al.* Characteristics of Adult Outpatients and Inpatients with COVID-19 - 11
421 Academic Medical Centers, United States, March-May 2020. *MMWR Morb Mortal Wkly Rep*
422 **69**, 841-846, doi:10.15585/mmwr.mm6926e3 (2020).
423 19 Klein, S. L. & Flanagan, K. L. Sex differences in immune responses. *Nat Rev Immunol* **16**, 626-
424 638, doi:10.1038/nri.2016.90 (2016).
425 20 Chakravarty, D. *et al.* Sex differences in SARS-CoV-2 infection rates and the potential link to
426 prostate cancer. *Commun Biol* **3**, 374, doi:10.1038/s42003-020-1088-9 (2020).

427   21   Jin, J. M. *et al.* Gender Differences in Patients With COVID-19: Focus on Severity and
428   Mortality. *Front Public Health* **8**, 152, doi:10.3389/fpubh.2020.00152 (2020).
429   22   Grifoni, A. *et al.* Targets of T Cell Responses to SARS-CoV-2 Coronavirus in Humans with
430   COVID-19 Disease and Unexposed Individuals. *Cell* **181**, 1489-1501 e1415,
431   doi:10.1016/j.cell.2020.05.015 (2020).
432   23   Peng, Y. *et al.* Broad and strong memory CD4(+) and CD8(+) T cells induced by SARS-CoV-2
433   in UK convalescent individuals following COVID-19. *Nat Immunol*, doi:10.1038/s41590-020-
434   0782-6 (2020).
435   24   Kaneko, N. *et al.* Loss of Bcl-6-Expressing T Follicular Helper Cells and Germinal Centers in
436   COVID-19. *Cell*, doi:10.1016/j.cell.2020.08.025 (2020).
437   25   Amanat, F. *et al.* A serological assay to detect SARS-CoV-2 seroconversion in humans. *Nat*
438   *Med* **26**, 1033-1036, doi:10.1038/s41591-020-0913-5 (2020).
439   26   Stadlbauer, D. *et al.* SARS-CoV-2 Seroconversion in Humans: A Detailed Protocol for a
440   Serological Assay, Antigen Production, and Test Setup. *Curr Protoc Microbiol* **57**, e100,
441   doi:10.1002/cpmc.100 (2020).
442